Electronic Supplementary Material (ESI) for Chemical Communications.

Supporting Information

Influence of Donor Point Modifications on the Assembly of Chalcogen-Bonded Organic Frameworks

Brian J. Eckstein,[a] Hannah R. Martin,[a] Michael P. Moghadasnia,[a] Arijit Halder,[a] Michael J. Melville,[a] Tara N. Buzinski,[a] Gary J. Balaich[b] and C. Michael McGuirk*[a]

[a]Department of Chemistry, Colorado School of Mines, Golden, Colorado, 80401, USA. *E-mail: cmmcguirk@mines.edu

[b]Department of Chemistry & Chemistry Research Center, Laboratories for Advanced Materials, United States Air Force Academy, Colorado Springs, Colorado, 80840, USA.

Table of Contents

S1. Materials synthesis

S1.1 General methods & reagents

Commercial reagents were used without further purification unless stated otherwise. Extra dry pyridine over molecular sieves was purchased from Thermo Scientific Chemicals. Anhydrous *N*,*N*-diisopropylethylamine (DIPEA) was purchased from TCI America. 200 Proof ethanol (EtOH) was purchased from Decon Laboratories, Inc. ACS grade acetone was purchased from Pharmco. ACS grade *N*,*N*-dimethylformamide (DMF) was purchased from Fischer Scientific. Selenium(IV) oxide (SeO_2), and tellurium(IV) chloride ($TeCl_4$) were purchased from Strem Chemicals, Inc. Deuterated dimethyl sulfoxide (DMSO-d_6) and deuterium oxide (D_2O) were purchased from Cambridge Isotope Laboratories. Potassium hydrogen phthalate was purchased from Sigma–Aldrich.

2,3,6,7,14,15-Hexaammoniumtriptycene hexachloride (**Trip6NH$_3$Cl**)[1, 2] and triptycene tris(1,2,5-selenadiazole) (**Trip3Sez**)[2] were prepared according to literature procedure. Note, the degree of solvation/hydration can vary between batches of **Trip6NH$_3$Cl**. Hence, effective molecular weights were established by quantitative ^{1}H NMR spectroscopy versus a potassium hydrogen phthalate standard in D_2O.

Unless otherwise noted, reactions were run under dry N_2 atmosphere using standard Schlenk techniques. ^{1}H and ^{13}C NMR spectra were collected on a JEOL ECA-500 spectrometer (500 MHz for ^{1}H NMR spectra and 125 MHz for ^{13}C spectra). The chemical shifts in the ^{1}H and ^{13}C NMR spectra are reported in parts per million (ppm) using the central residual solvent peaks as an internal standard. Mass measurement was performed using a Bruker UltrafleXtreme MALDI-TOF/TOF mass spectrometer. Compounds were deposited on ground steel target plates from either solutions or powdered suspensions in anhydrous THF. Mass data was obtained in positive mode laser desorption ionization without matrix (LDI+) using an 80 ns extraction delay.

S1.2 ***Trip2Sez1Tez*** *and* ***Trip1Sez2Tez*** *tecton synthesis*

Scheme S1. General Route to Trip2Sez2NH$_2$ and Trip1Sez4NH$_2$ from Trip6NH$_3$Cl

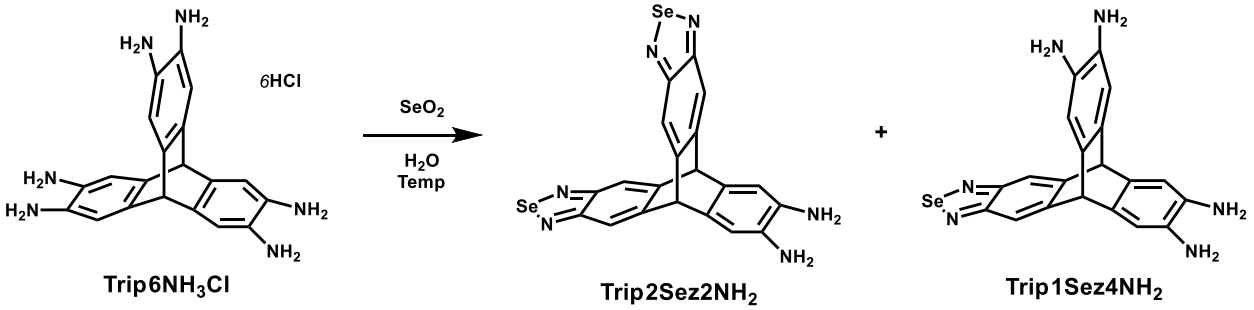

*S1.2.1 Triptycene bis(1,2,5-selenadiazole) diamine (****Trip2Sez2NH$_2$****)*

A solution of **Trip6NH$_3$Cl** (2.01 g, 3.49 mmol) in 18 mL deionized water (DI H_2O) was heated to reflux in a 100 mL round bottom flask, then a solution of SeO_2 (819 mg, 7.38 mmol, 2.12 equiv.) in 18 mL DI H_2O was added dropwise over 10 min, producing a yellow suspension. The reaction mixture was subsequently refluxed for 21 h then cooled to room temperature. A yellow solid was collected by vacuum filtration and washed with DI H_2O (3x20 mL). To neutralize HCl produced during the reaction, the crude solid was dispersed in 40 mL of a saturated $NaHCO_3$ (aq) solution, producing a red–orange suspension. Once all bubbling subsided, the free-base crude

was collected by vacuum filtration, washed with DI H_2O (3x30 mL) then MeOH (3x30 mL). The crude was purified by dissolving in 30 mL of boiling DMF then precipitating the hot solution into 200 mL of chloroform while stirring vigorously. Once cooled to room temperature, the precipitate was collected by vacuum filtration, washed with cold chloroform (3x30 mL), then dried under vacuum at 80 °C overnight to afford the product as a red–orange powder (1.15 g, 2.32 mmol, 66.4 % yield). ^{1}H NMR (500 MHz, DMSO-d_6) δ 7.74 (s, 4H), 6.71 (s, 2H), 5.53 (s, 2H), 4.53 (s, 4H); ^{13}C NMR (126 MHz, DMSO-d_6) δ 159.19, 145.08, 133.63, 129.69, 115.70, 110.66, 50.50; MS (LDI+) m/z: $[M+H]^+$ calcd. for $C_{20}H_{13}N_6Se_2$ 496.95, found 496.9.

*S1.2.2 Triptycene mono(1,2,5-selenadiazole) tetraamine (**Trip1Sez4NH$_2$**)*

A solution of **Trip6NH$_3$Cl** (4.45 g, 5.98 mmol) in 12 mL deionized water (DI H_2O) was stirred at room temperature in a 250 mL round bottom flask, then a solution of SeO_2 (1.13 g, 10.2 mmol, 1.7 equiv.) in 68 mL DI H_2O was added dropwise over 10 min, producing a yellow suspension. The reaction mixture was then allowed to stir at room temperature for an additional 21 h. The crude solid was collected by vacuum filtration then combined with 300 mL of a 0.06 M HCl solution, which was then sonicated for 1 hr then stirred at 75 °C for 6 hr. After cooling to room temperature, the precipitate was removed. The collected filtrate was neutralized with saturated $NaHCO_3$ (aq) solution producing an orange precipitate that was collected by vacuum filtration, washed with deionoized water then 200 proof ethanol, and then dried under vacuum at 80 °C overnight to afford the product as an orange powder (0.651 g, 1.55 mmol, 26.0 % yield). ^{1}H NMR (500 MHz, DMSO-d_6) δ 7.45 (s, 2H), 6.60 (s, 4H), 5.00 (s, 2H), 4.29 (s, 8H); ^{13}C NMR (126 MHz, DMSO-d_6) δ 159.45, 148.32, 132.86, 132.18, 113.49, 110.71, 50.69; MS (LDI+) m/z: $[M+H]^+$ calcd. for $C_{20}H_{17}N_6Se$ 421.07, found 421.1.

Scheme S2. Route to Trip2Sez1Tez from Trip2Sez2NH$_2$

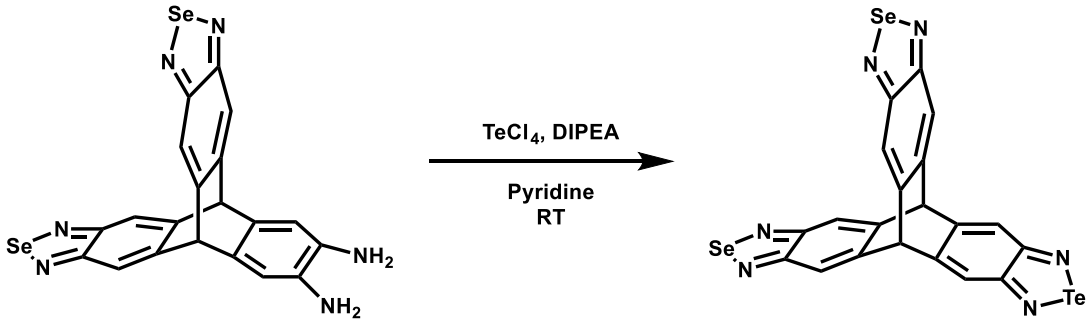

*S1.2.3 Triptycene bis(1,2,5-selenadiazole) mono(1,2,5-telluradiazole) (T**rip2Sez1Tez**)*

A suspension of **Trip2Sez2NH$_2$** (314.0 mg, 0.365 mmol) in 16 mL anhydrous pyridine was stirred at room temperature in a 100 mL round bottom flask under nitrogen atmosphere, then a suspension of $TeCl_4$ (179.2 mg, 0.665 mmol, 1.05 equiv.) in 16 mL anhydrous pyridine was added dropwise over 15 min. The resultant dark amber solution was stirred for 10 min, then *N*,*N*-diisopropylethylamine (0.65 mL, 6.8 mmol, 11 equiv.) was added dropwise over 2 min. The resultant orange–yellow suspension was stirred for 10 min then pipetted into 150 mL dry toluene stirring in a 250 mL Erlenmeyer flask. The precipitate was isolated by vacuum filtration, washed with acetone, then dried under vacuum at 70 °C overnight to afford the product as an orange–yellow powder (0.378 g, 0.611 mmol, 96.2 % yield). ^{1}H NMR (500 MHz, DMSO-d_6) δ 7.95 (s,

4H), 7.62 (s, 2H), 5.97 (s, 2H); MS (LDI+) m/z: $[M+H]^+$ calcd. for $C_{20}H_9N_6Se_2Te$ 622.83, found 622.7.

Scheme S3. Route to Trip1Sez2Tez from Trip1Sez4NH$_2$

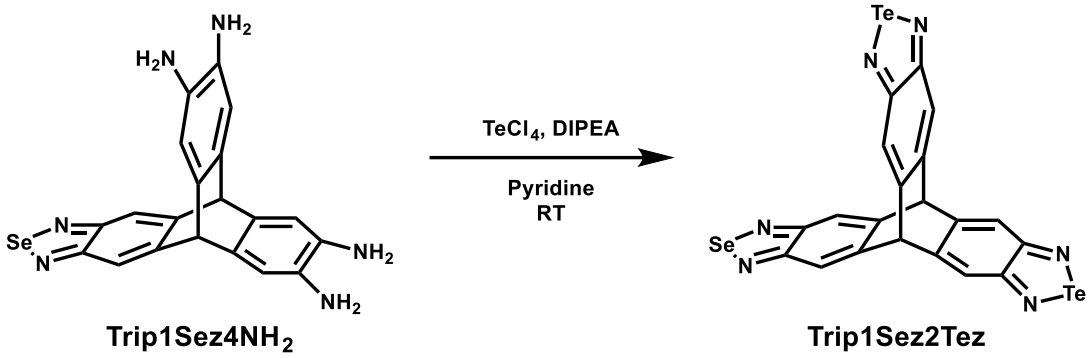

Trip1Sez4NH$_2$ **Trip1Sez2Tez**

*S1.2.4 Triptycene mono(1,2,5-selenadiazole) bis(1,2,5-telluradiazole) (T**rip1Sez2Tez**)*

A suspension of **Trip1Sez4NH$_2$** (439.8 mg, 1.05 mmol) in 150 mL anhydrous pyridine was stirred at room temperature in a 500 mL round bottom flask under nitrogen atmosphere, then a suspension of $TeCl_4$ (565.9 mg, 2.10 mmol, 2.00 equiv.) in 35 mL anhydrous pyridine was added dropwise over 15 min. The resultant dark amber solution was stirred for 10 min, then N,N-diisopropylethylamine (2.9 mL, 16.8 mmol, 16 equiv.) was added dropwise over 2 min. The resultant orange–yellow suspension was stirred for 1 hr. The precipitate was isolated by vacuum filtration, washed with anhydrous pyridine then acetone, and dried under vacuum at 70 °C overnight to afford the product as an orange–yellow powder (0.631 g, 0.946 mmol, 90.1 % yield). ^{1}H NMR (500 MHz, DMSO-d_6) δ 7.92 (s, 2H), 7.60 (s, 4H), 5.85 (s, 2H). Note that the low solubility of **Trip1Sez2Tez** in DMSO necessitates ≥ 256 scans to achieve appreciable S/N and makes it impossible establish potential impurities versus external contaminants. MS (LDI+) m/z: $[M+H]^+$ calcd. for $C_{20}H_9N_6Se_1Te_2$ 672.82, found 672.8.

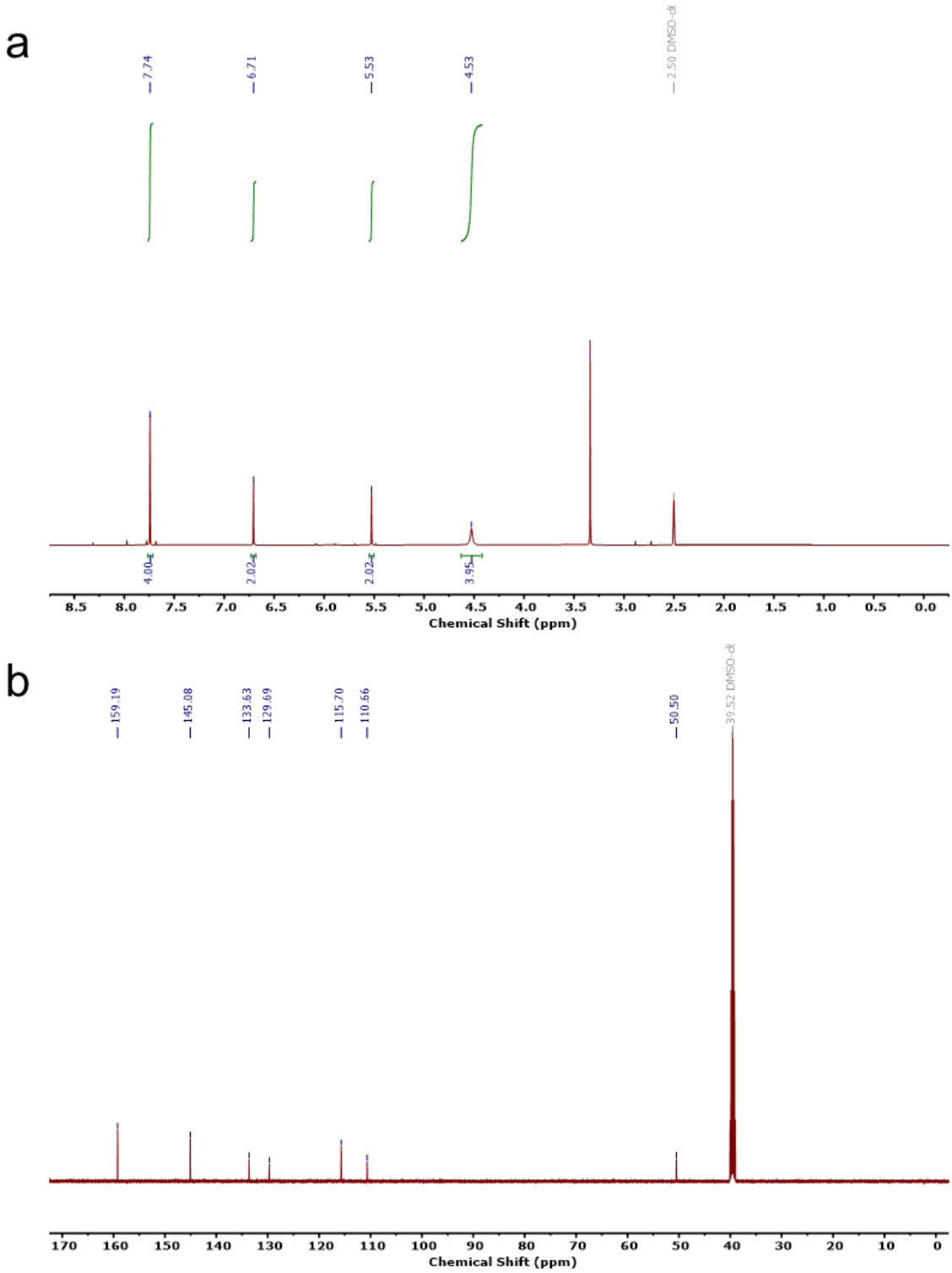

Figure S1. (a) ^{1}H and (b) ^{13}C NMR spectra of **Trip2Sez2NH$_2$** in DMSO-*d*$_6$.

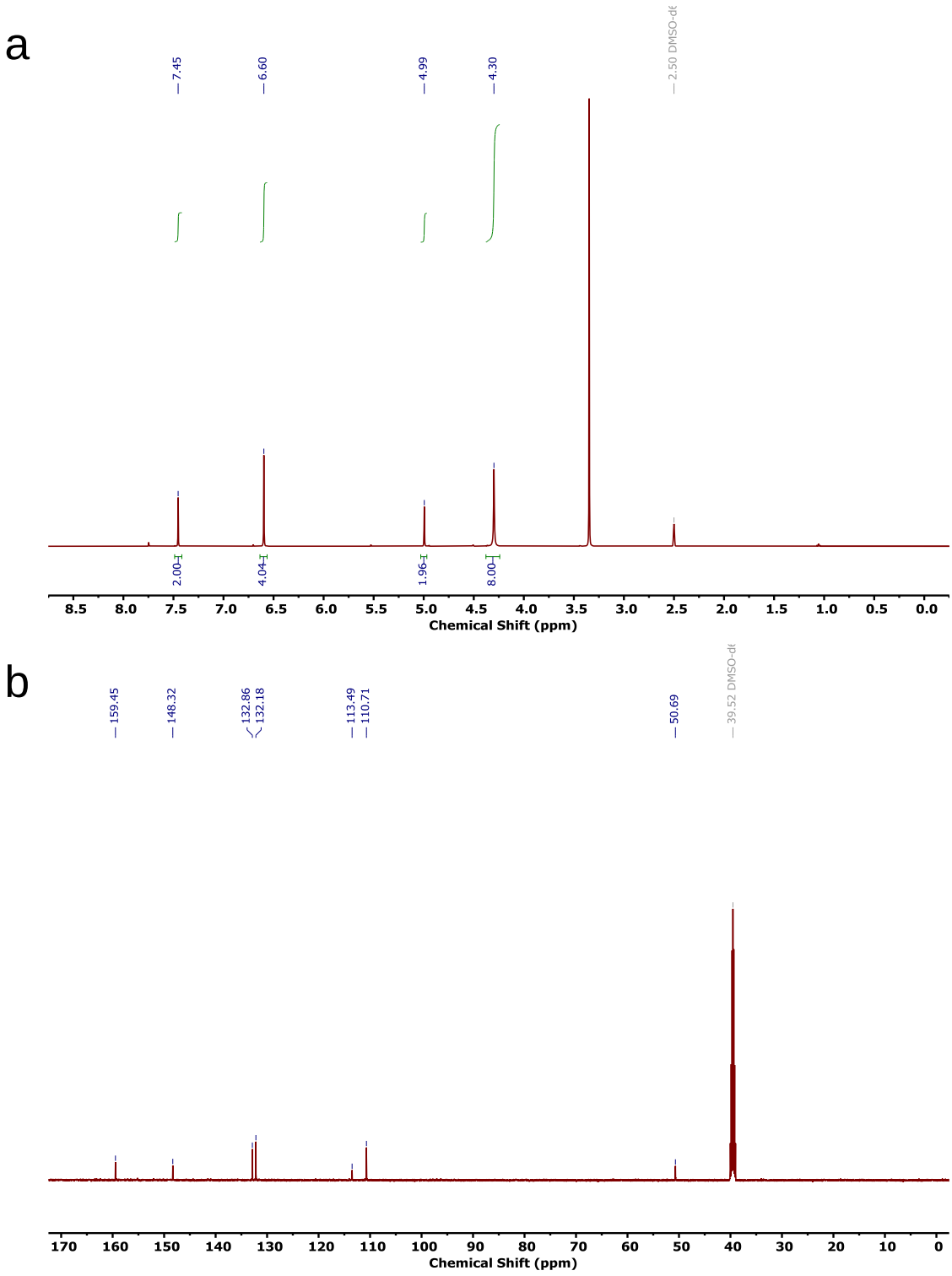

Figure S2. (a) ^{1}H and (b) ^{13}C NMR spectra of **Trip1Sez4NH$_2$** in DMSO-d_6.

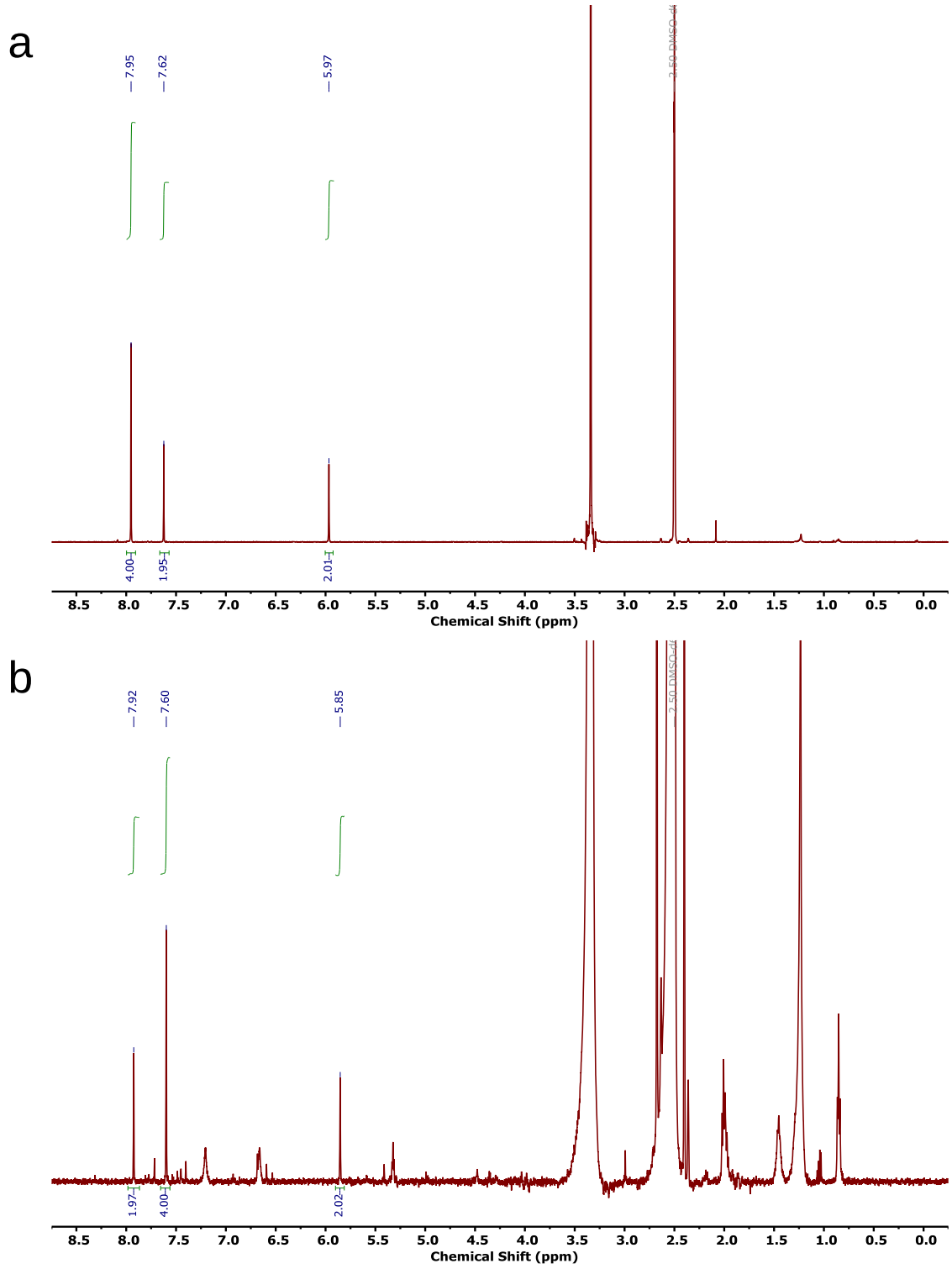

Figure S3. ^{1}H NMR spectra of (a) **Trip2Sez1Tez** and (b) **Trip1Sez2Tez** in DMSO-d_6. Note, due to the poor solubility of both **Trip2Sez1Tez** and **Trip1Sez2Tez**, we were unable to collect suitable ^{13}C NMR data for either compound.

S2. Trip2Sez1Tez & Trip1Sez2Tez crystallization experiments

S2.1 *General methods & reagents*

All crystallization experiments were conducted under ambient atmosphere conditions unless noted otherwise. Commercial solvents were used without any further purification. Anhydrous dimethyl sulfoxide (DMSO), anhydrous 1-methyl-2-pyrrolidinone (NMP), and 1-chloronaphthalene (CN) were purchased from Sigma–Aldrich.

S2.2 ***Trip2Sez1Tez*** *single crystal growth procedures*

S2.2.1 DMSO-grown ***Trip2Sez1Tez****-VI*

4 mL glass vials were loaded with ~2 mg of **Trip2Sez1Tez** and ~1 mL anhydrous DMSO was added to reach a target concentration of 2 mg/mL. The vials were sealed with PTFE-lined screw caps, heated in an aluminum block at 150 °C until all solid material dissolved, then allowed to cool slowly to room temperature in the aluminum block. After sitting undisturbed overnight (~18 hr), **Trip2Sez1Tez**-*VI* was found to have crystallized as mm-scale orange plates.

S2.2.2 CN–DMSO-grown ***Trip2Sez1Tez****-I*

4 mL glass vials were loaded with ~3 mg of **Trip2Sez1Tez** and ~1 mL of a 1:4 (v/v) CN to anhydrous DMSO solvent mixture was added to reach a target concentration of 3 mg/mL. The vials were sealed with PTFE-lined screw caps, heated in an aluminum block at 150 °C until all solid material dissolved, then allowed to cool slowly to room temperature in the aluminum block. After sitting undisturbed overnight (~18 hr), **Trip2Sez1Tez**-*I* was found to have crystallized as mm-scale yellow needles.

S2.2.3 NMP-grown ***Trip2Sez1Tez****-I*

4 mL glass vials were loaded with ~3-4 mg of **Trip2Sez1Tez** and ~1 mL of anhydrous NMP was added to reach a target concentration of 3-4 mg/mL. The vials were sealed with PTFE-lined screw caps, heated in an aluminum block at 150 °C until all solid material dissolved, then allowed to cool slowly to room temperature in the aluminum block. After sitting undisturbed overnight (~18 hr), **Trip2Sez1Tez**-*I* was found to have crystallized as mm-scale orange–yellow rods.

S2.3 Batch-scale crystallization procedures

S2.3.1 ***Trip2Sez1Tez****-VI*

A 20 mL glass vial was loaded with 50 mg of **Trip2Sez1Tez** and 5 mL anhydrous DMSO was added to reach a concentration of 10 mg/mL. The vial was sealed with a PTFE-line screw cap, heated on a hot plate set to 190 °C until all solid material dissolved, then allowed to cool quickly by removing from the hot plate. Within minutes of reaching room temperature, a plethora of small orange **Trip2Sez1Tez**-*VI* plates had crystallized from solution.

S2.3.2 ***Trip2Sez1Tez****-I*

A 125 mL Erlenmeyer flask was loaded with 210 mg of **Trip2Sez1Tez** and 30 mL of a 1:4 (v/v) CN to anhydrous DMSO solvent mixture was added to reach a concentration of 7 mg/mL. The flask was sealed with a rubber septum, heated on a hot plate set to 180 °C until all solid

material dissolved, then allowed to cool quickly by removing from the hot plate. Within minutes of reaching room temperature, a plethora of small yellow **Trip2Sez1Tez**-*I* needles had crystallized from solution.

S2.3.3 ***Trip1Sez2Tez****-I*

A 250 mL Erlenmeyer flask with a stir bar was loaded with 625 mg **Trip1Sez2Tez** and 125 mL anhydrous DMSO was added to reach a concentration of 5 mg/mL. The flask was sealed with a rubber septum and put under N_2 atmosphere using a Schlenk line. The suspension was stirred and heated on a hot plate set to 225 °C until all solid material dissolved. Then, stirring was stopped and the hot plate was set to 150 °C for two hours followed by 100 °C for two hours before allowing to slowly cool to room temperature. Within minutes of cooling from 225 °C, fine yellow **Trip2Sez1Tez**-*I* needles began crystallizing from solution.

S2.4 Digital images of the ***Trip2Sez1Tez*** *and* ***Trip1Sez2Tez*** *crystals*

Digital images of the **Trip2Sez1Tez** crystals were captured with an AmScope UHM350-11 tabletop digital microscope. The digital image of the **Trip1Sez2Tez**-*I* crystals was captured using a Keyence VHX-5000 digital microscope.

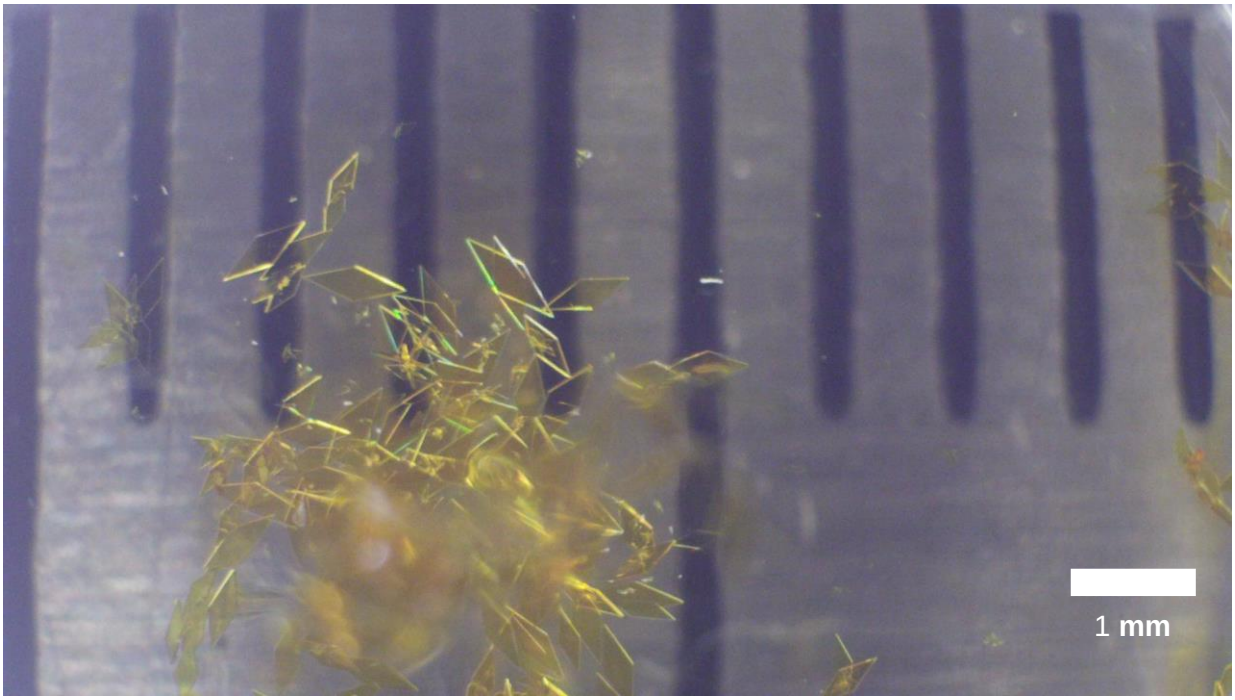

Figure S4. Digital image of as-grown **Trip2Sez1Tez**-*VI* in DMSO showing the plate-like crystal morphology.

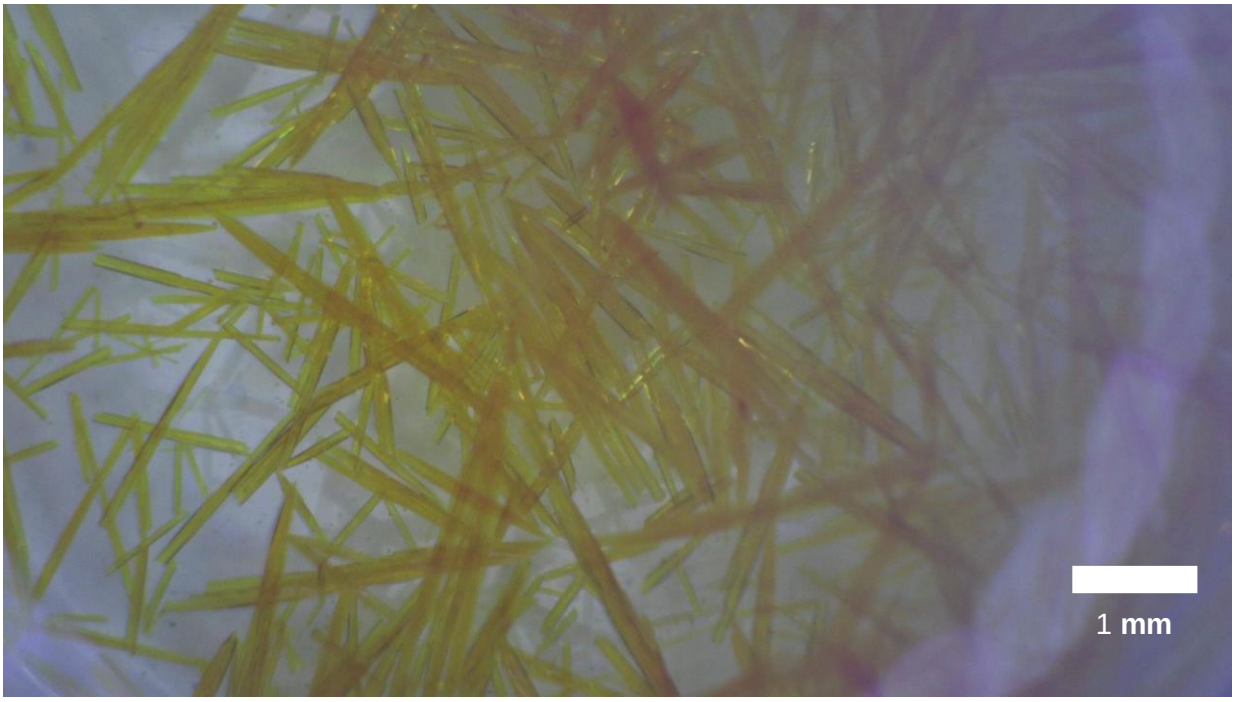

Figure S5. Digital image of as-grown **Trip2Sez1Tez**-*I* in CN–DMSO showing the rod/needle crystal morphology.

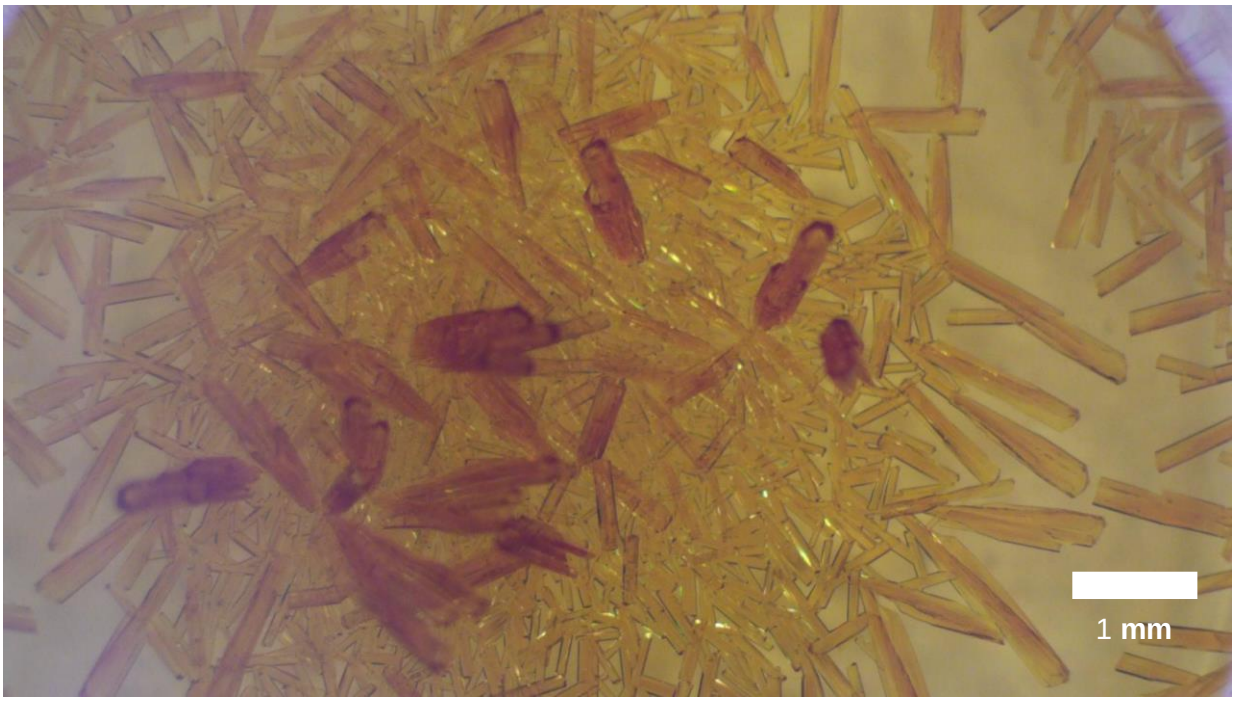

Figure S6. Digital image of as-grown **Trip2Sez1Tez**-*I* in NMP showing the rod/needle crystal morphology.

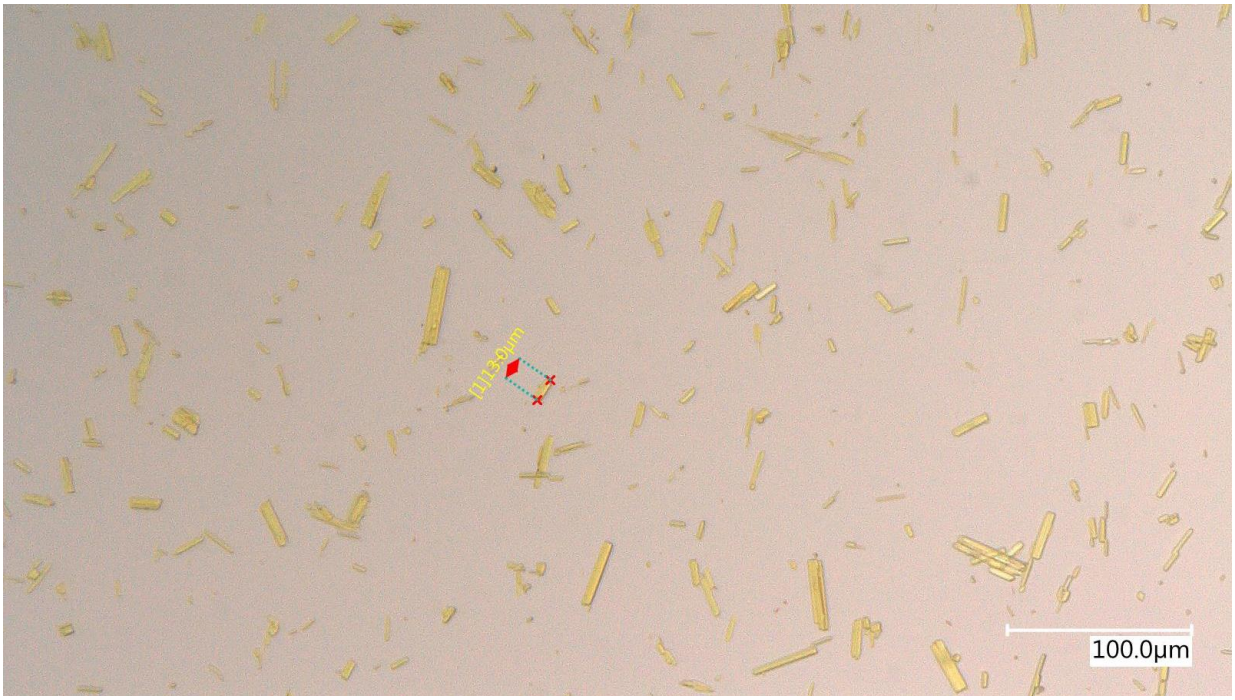

Figure S7. Digital image of as-grown **Trip1Sez2Tez**-*I* in DMSO showing the needle-like crystal morphology.

S3. X-ray crystallographic analyses

S3.1 Single-crystal X-ray diffraction (SCXRD) data collection and processing procedures

The data collection for SCXRD studies of the **Trip2Sez1Tez** single crystals were carried out using one of two methods.

Method A: The X-ray intensity data were measured on a Rigaku Synergy-i single crystal diffractometer equipped with a Mo Kα radiation source (λ = 0.71073 Å) and a Bantam HyPIX-3000 direct photon counting detector.

Method B: The X-ray intensity data were measured on a Rigaku XtaLAB Synergy R, DW system, HyPix single crystal diffractometer equipped with a rotating anode Cu Kα radiation source (λ = 1.54184 Å).

The data were integrated with the CrysAlisPro software program[3] and corrected for absorption effects using an empirical correction implemented in the SCALE 3 ABSPACK software program as well as a numerical absorption correction based on Gaussian integration over a multifaceted crystal model. The structures were solved by direct methods with SHELXT[4] and refined by full-matrix least-squares on $|F|^2$ with SHELXL[5] in the Olex2 software package.[6] All non-hydrogen atoms were refined anisotropically, and hydrogen atoms were placed relative to their parent atom using AFIX instructions in SHELXL. In the final refinement steps, void spaces occupied by disordered solvent molecules with unmappable electron density were treated using the PLATON/SQUEEZE[7] or the Olex2 masking function as detailed in the corresponding CIF files.

ORTEP representations of the non-equivalent molecules in the unit cells of the structures reported here were generated using the program Mercury developed by the Cambridge Crystallographic Data Centre (CCDC).[8]

S3.1.1 Additional data reduction and refinement procedures for ***Trip2Sez1Tez****-VI*

The **Trip2Sez1Tez**-*VI* SCXRD data was collected on a merohedral twinned crystal with domains related by the twin law (-1, 0, -1, 0, -1, 0, 0, 0, 1), i.e., a twofold rotation about the *c*-axis. The twinning was identified and treated in Olex2 during refinement. Additionally, increasing the integration mask size by a factor of 1.5 then discarding frames with $R_{int} > 0.1$ during data reduction and applying the RIGU rigid body restraint to the asymmetric unit during refinement afforded the best R values for the structure.

S3.2 SCXRD structure data and refinement details for as-grown ***Trip2Sez1Tez****-VI and -I*

Note, the data collection method used for each structure is indicated in its respective subheading below.

*S3.2.1 DMSO-solvated **Trip2Sez1Tez**-VI (Method A)*

Table S1. Crystallographic details for DMSO-solvated Trip2Sez1Tez-*VI*

Identification code	Trip2Sez1Tez-VI _DMSO_140K
Chemical formula	$C_{20}H_8N_6Se_2Te_1$
Formula weight	617.84 g/mol
Temperature	139.99(10) K
Crystal system	monoclinic
Space group	C2/*c*
Unit cell dimensions	a = 12.5050(3) Å; b = 36.9387(7) Å; c = 7.7404(2) Å α = 90°; β = 107.994(3)°; γ = 90°
Volume	3400.57(15) $Å^3$
Z	4
Density (calculated)	1.207 g/cm^3
Absorption coefficient	3.027 mm^{-1}
F(000)	1160.0
Crystal size	0.506 x 0.264 x 0.018 mm^3
Radiation	Mo K_α (λ = 0.71073 Å)
θ range for data collection	1.799 to 26.7°
Index ranges	$-15 \leq h \leq 14$; $-46 \leq k \leq 46$; $-9 \leq l \leq 9$
Reflections collected	20625
Independent reflections	3451 [R(int) = 0.0305]
Data / restraints / parameters	3451 / 102 / 133
Goodness-of-fit on F^2	1.123
Final R indexes [$I \geq 2\sigma(I)$]	R_1 = 0.0606, wR_2 = 0.1636
Final R indexes [all data]	R_1 = 0.0688, wR_2 = 0.1667
Largest diff. peak / hole	1.78 / -2.47 e $Å^{-3}$

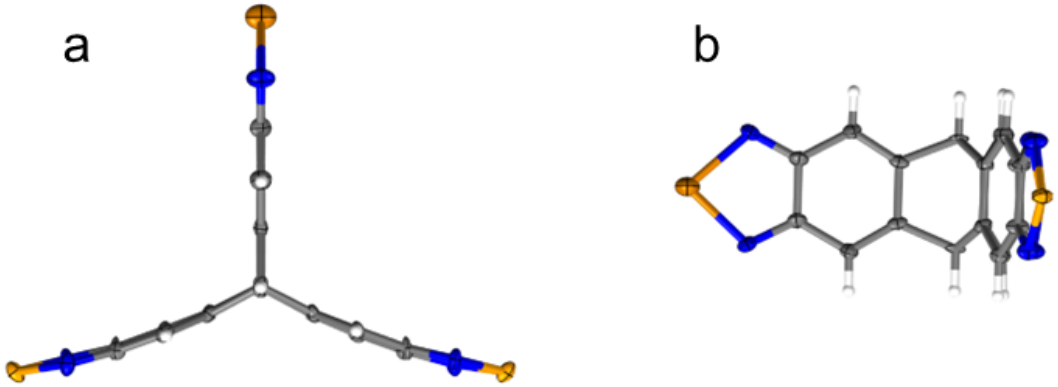

Figure S8. ORTEP representation of **Trip2Sez1Tez** in DMSO-solvated **Trip2Sez1Tez**-*VI* at 140 K viewed along (a) the [001] and (b) [201] unit cell directions. Orange, gold, grey, and blue thermal ellipsoids (shown at the 50% probability level) represent Te, Se, C, and N atoms, respectively, and H atoms are represented as white spheres.

*S3.2.2 CN–DMSO-solvated **Trip2Sez1Tez**-I (Method B)*

Table S2. Crystallographic details for CN–DMSO-solvated Trip2Sez1Tez-*I*

Identification code	Trip2Sez1Tez-I_CN-DMSO_100K
Empirical formula	$C_{20}H_8N_6Se_2Te$
Formula weight	617.84
Temperature / K	100.1(3)
Crystal system	hexagonal
Space group	$P6_3/mmc$
Unit cell dimensions	a = b = 21.529(3) Å; c = 7.6530(6) Å α = β = 90°; γ = 120°
Volume	3072.0(8) $Å^3$
Z	2
Density (calculated)	0.668 g/cm^3
Absorption coefficient	5.230 mm^{-1}
F(000)	580
Crystal size / mm^3	0.236 × 0.015 × 0.005 mm^3
Radiation	Cu K_α (λ = 1.54184 Å)
θ range for data collection	2.37 to 79.087°
Index ranges	$-26 \le h \le 26$; $-23 \le k \le 26$; $-6 \le l \le 9$
Reflections collected	18510
Independent reflections	1278 [R(int) = 0.1056]
Data / restraints / parameters	1278 / 0 / 36
Goodness-of-fit on F^2	1.112
Final R indexes [I≥2σ(I)]	R_1 = 0.0844, wR_2 = 0.2314
Final R indexes [all data]	R_1 = 0.0913, wR_2 = 0.2377
Largest diff. peak / hole	0.329 / -1.683 e $Å^{-3}$

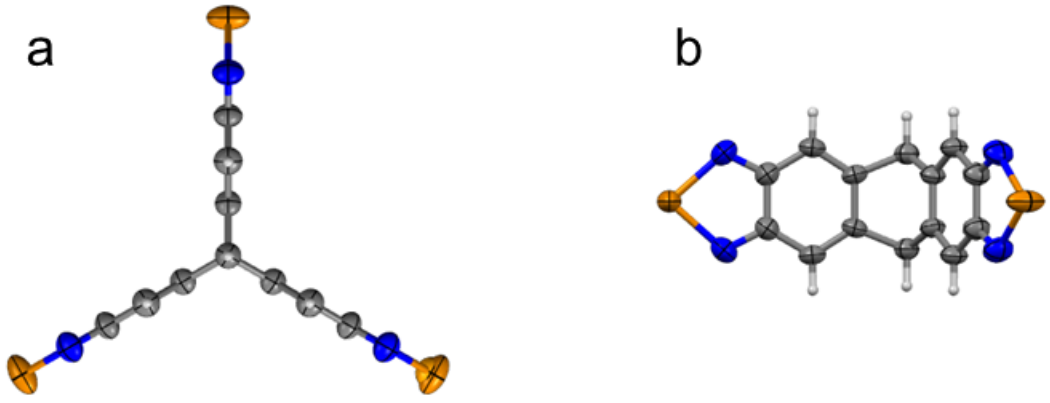

Figure S9. ORTEP representation of **Trip2Sez1Tez** in CN–DMSO-solvated **Trip2Sez1Tez-*I*** at 100 K viewed along (a) the [001] and (b) [100] unit cell directions. Orange, gold, grey, and blue thermal ellipsoids (shown at the 50% probability level) represent Te, Se, C, and N atoms, respectively, and H atoms are represented as white spheres.

*S3.2.3 NMP-solvated **Trip2Sez1Tez**-I (Method B)*

Table S3. Crystallographic details for NMP-solvated Trip2Sez1Tez-*I*

Identification code	Trip2Sez1Tez-I_NMP_100K
Empirical formula	$C_{20}H_8N_6Se_2Te$
Formula weight	617.84
Temperature / K	100.1(3)
Crystal system	hexagonal
Space group	$P6_3/mmc$
Unit cell dimensions	a = b = 21.6560(4) Å; c = 7.6612(2) Å α = β = 90°; γ = 120°
Volume	3111.60(14) Å^3
Z	2
Density (calculated)	0.659 g/cm^3
Absorption coefficient	5.164 mm^{-1}
F(000)	580
Crystal size / mm^3	0.507 × 0.063 × 0.034 mm^3
Radiation	Cu K_α (λ = 1.54184 Å)
θ range for data collection	2.356 to 78.19°
Index ranges	-27 ≤ h ≤ 27; -27 ≤ k ≤ 27; -7 ≤ l ≤ 9
Reflections collected	45260
Independent reflections	1291 [R(int) = 0.0498]
Data / restraints / parameters	1291 / 0 / 36
Goodness-of-fit on F^2	1.100
Final R indexes [I≥2σ(I)]	R_1 = 0.0794, wR_2 = 0.1780
Final R indexes [all data]	R_1 = 0.0795, wR_2 = 0.1781
Largest diff. peak / hole	0.999 / -1.035 e Å^{-3}

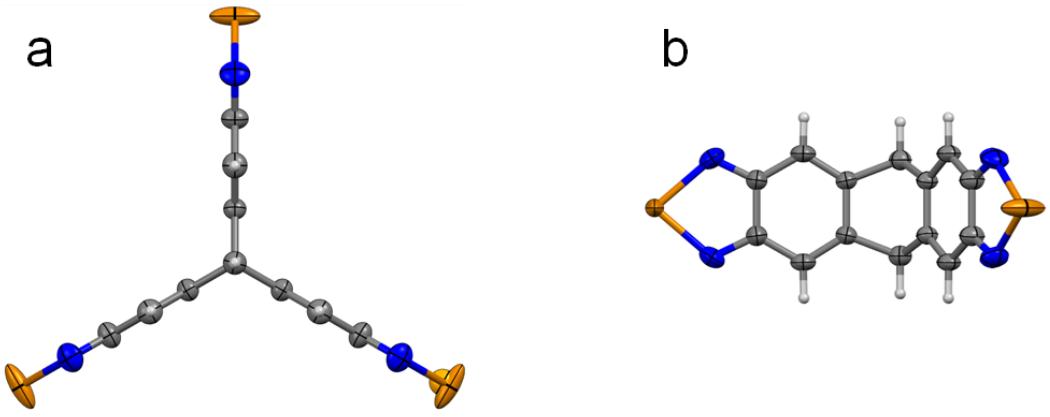

Figure S10. ORTEP representation of **Trip2Sez1Tez** in NMP-solvated **Trip2Sez1Tez-*I*** at 100 K viewed along (a) the [001] and (b) [100] unit cell directions. Orange, gold, grey, and blue thermal ellipsoids (shown at the 50% probability level) represent Te, Se, C, and N atoms, respectively, and H atoms are represented as white spheres.

*S3.3 Chalcogen atom disorder model for **Trip2Sez1Tez**-I and **Trip1Sez2Tez**-I structures*

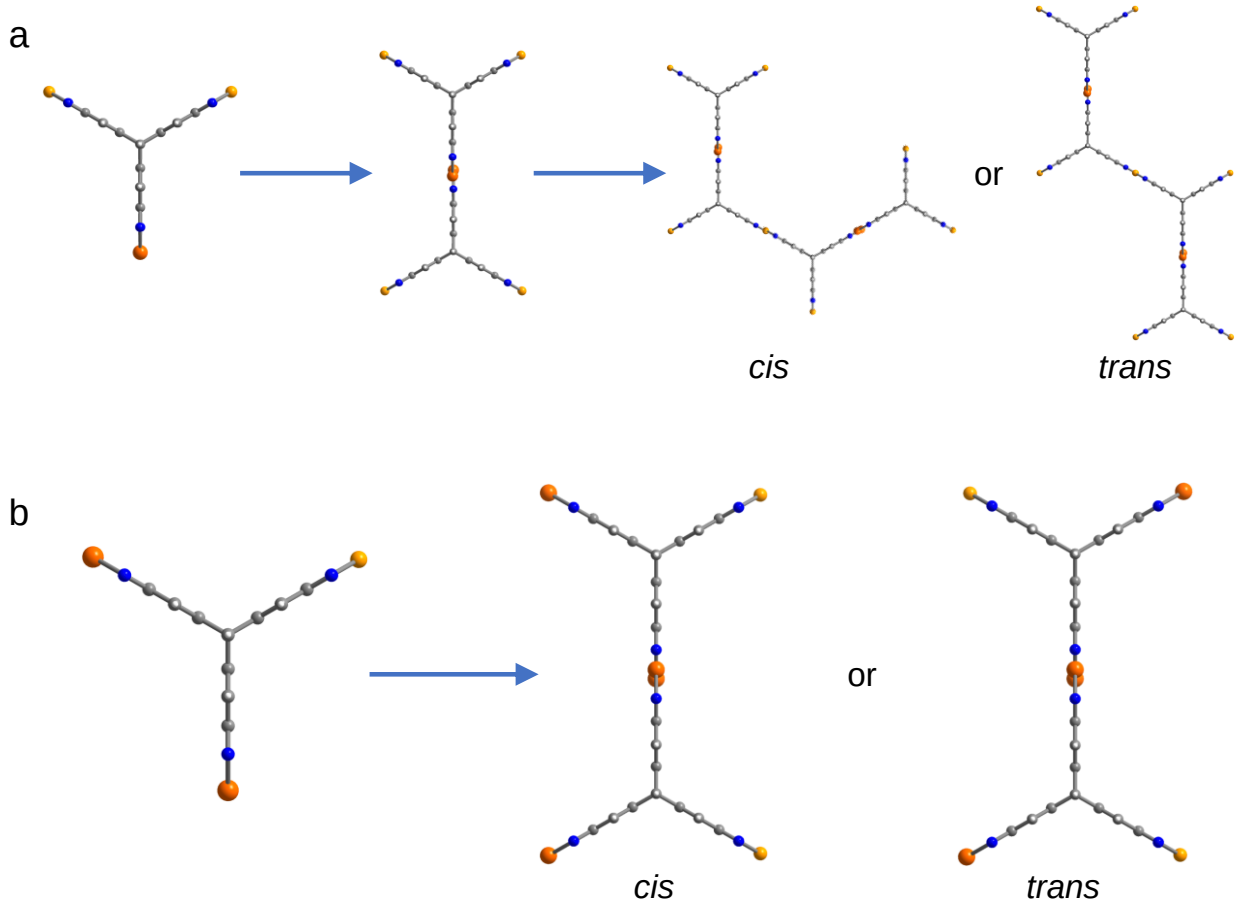

Figure S11. The Ch-bonding assembly of both (a) **Trip2Sez1Tez** and (b) **Trip1Sez2Tez** can ostensibly proceed through both *cis*- and *trans*-like configurations that, if coincident, would give rise to disordered distributions of Tez and Sez ribbon motifs within the respective **Trip2Sez1Tez**-*I* and **Trip1Sez2Tez**-*I* structures.

S3.4 Powder X-ray diffraction (PXRD) procedures

PXRD data was collected on a Bruker D2 Phaser diffractometer with Cu K_α radiation (λ = 1.54184 Å) outfitted with a 1 mm knife edge. Data was acquired over a 2θ range of 3–30° with a step size and duration of 0.02° and 1 sec, respectively, and the sample stage was rotated at a rate of 2π rad/min.

Samples were prepared on the D2 Phaser silicon (Si) substrates by one of two methods depending on the sample state.

Wet (e.g., as-grown crystals or solvent exchange samples): Excess supernatant was removed, and the crystals were mechanically crushed to improve homogeneity and limit potential orientational effects. The resultant suspensions or pastes were then deposited on the Si substrates and spread around to achieve smooth, even coverage. Excess solvent was allowed to evaporate or, in the case of high boiling point solvents, was carefully sponged up using cellulose filter paper.

Dry: A thin layer of petroleum jelly was deposited onto the surface of the Si substrates to serve as an adhesive. Powders were carefully dispersed across the substrate then gently pressed using weigh paper to achieve even, smooth sample coverage.

S4. Porosity characterization

S4.1 Solvent exchange and activation

S4.1.1 General methods

Solvent exchanges were carried out by removing supernatant, adding fresh solvent, then letting the sample sit for 24 hrs. Five such exchanges were performed with each solvent before moving on to the next stage.

Activations (i.e., complete solvent removal) were performed by removing the last exchange supernatant and allowing the last residual amounts of solvent to evaporate for 3–5 days under Schlenk line N_2 atmosphere. An active N_2 purge was applied for 24–48 hr to further drive off solvent before vacuum was used to remove any remaining labile solvent guest molecules.

Over the course of the solvent exchange and activation procedures, samples were taken for PXRD and NMR spectroscopy experiments to characterize the crystalline structure and presence of solvent guests, respectively. Note, **Trip1Sez2Tez**-*I* samples for NMR spectroscopy analysis could not be completely dissolved in DMSO-d_6 and thus were gently heated and stirred for 30–60 min then sonicated to promote extraction of the solvent guest molecules into the NMR solution.

S4.1.2 Reagents

ACS grade acetone was purchased from Pharmco. *n*-Pentane was purchased from Fischer Scientific. Acetonitrile (ACN) was purchased from Fischer Scientific and dried over calcium hydride. Diethyl ether (Et_2O) was purchased from Sigma–Aldrich and further purified in a LC Tech solvent system.

*S4.1.3 Solvent exchange characterization with **Trip2Sez1Tez**-VI*

Note, we initially attempted acetone exchange, but significant coloration of the supernatant suggested decomposition. Hence, anhydrous ACN and Et_2O were used instead.

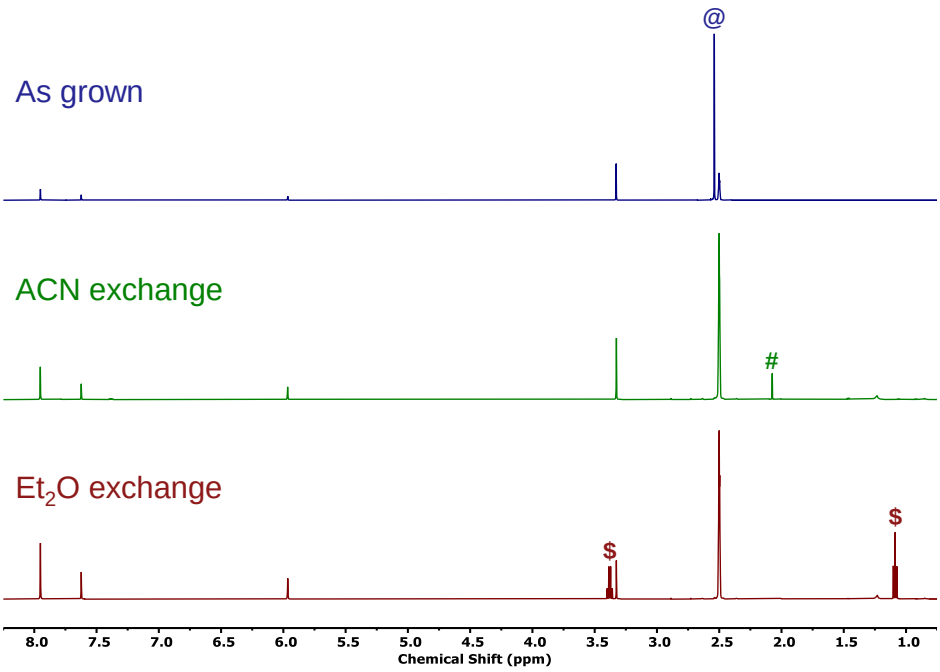

Figure S12. Stacked [1]H NMR spectra from **Trip2Sez1Tez**-*VI* samples taken as grown from DMSO, after 5 exchange cycles with ACN, and after 5 exchange cycles with Et2O. The signals of the DMSO, ACN, and Et_2O guest molecules are indicated by @, #, and $ symbols, respectively.

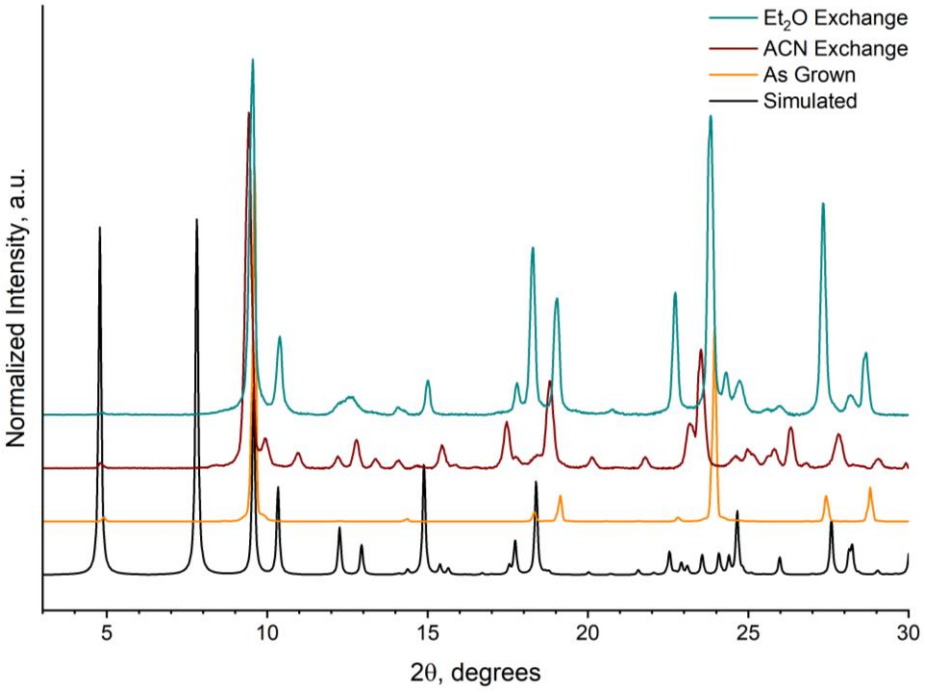

Figure S13. Stacked PXRD patterns of **Trip2Sez1Tez**-*VI* samples taken as grown from DMSO, after 5 exchange cycles with ACN, and after 5 exchange cycles with Et_2O. The simulated pattern from the **Trip2Sez1Tez**-*VI* crystal structure is included for reference.

*S4.1.4 Solvent exchange and activation characterization for **Trip2Sez1Tez**-I*

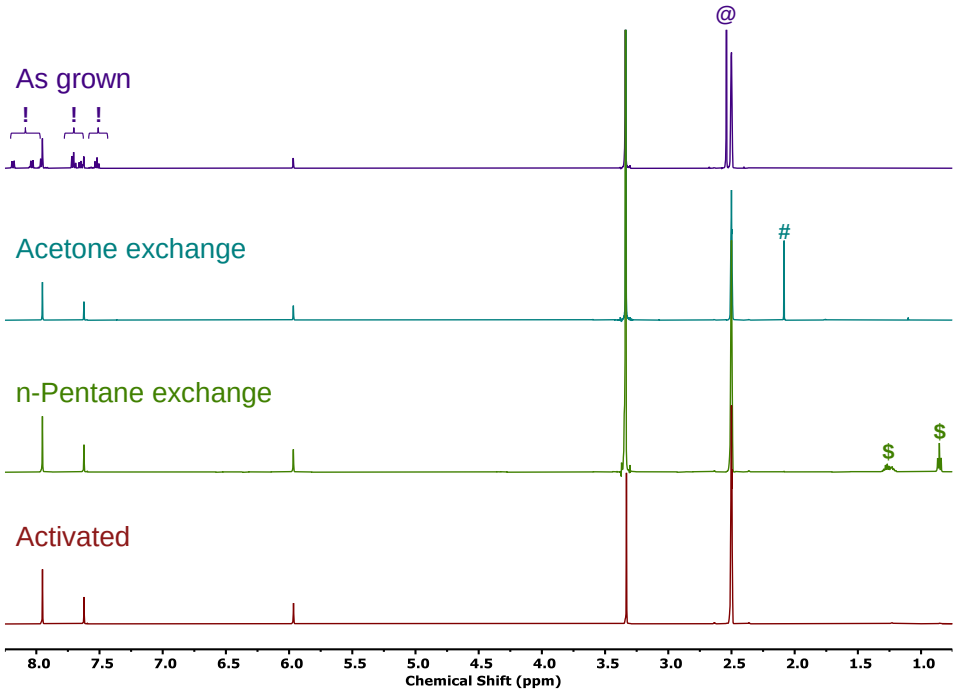

Figure S14. Stacked ^{1}H NMR spectra from **Trip2Sez1Tez**-*I* samples taken as grown from CN–DMSO, after 5 exchange cycles with acetone, after 5 exchange cycles with *n*-pentane, and after activation. The signals of the CN, DMSO, acetone, and n-pentane guest molecules are indicated by !, @, #, and $ symbols, respectively.

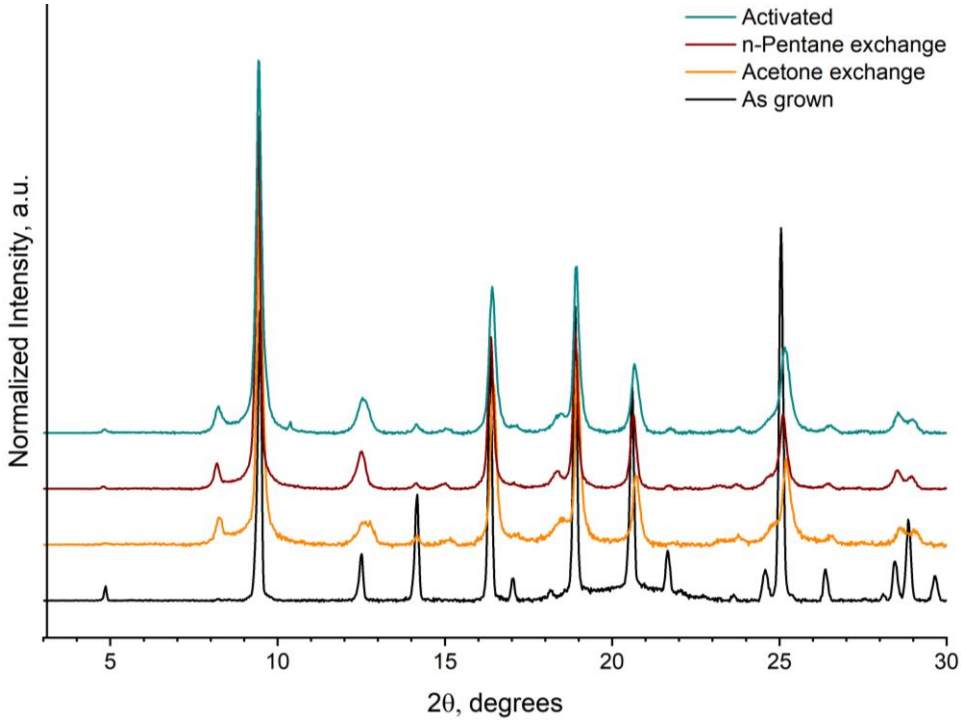

Figure S15. Stacked PXRD patterns of **Trip2Sez1Tez**-*I* samples taken as grown from CN–DMSO, after 5 exchange cycles with acetone, after 5 exchange cycles with *n*-pentane, and after activation.

S4.1.5 Solvent exchange and activation characterization for ***Trip1Sez2Tez****-I*

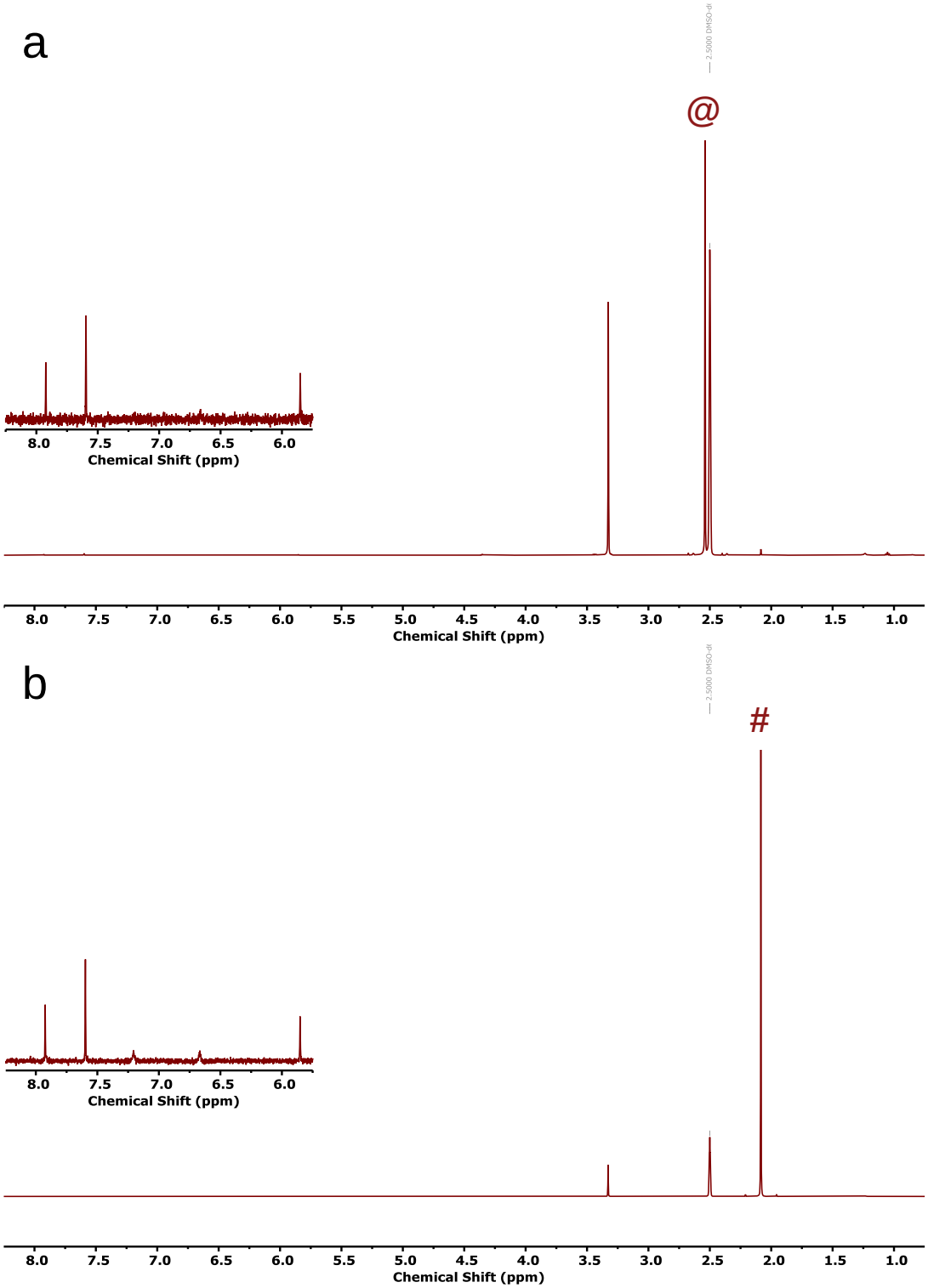

Figure S16. ^{1}H NMR spectra of **Trip1Sez2Tez***-I* samples taken (a) as grown from DMSO and (b) after 5 exchange cycles with acetone. The signals of DMSO and acetone guest molecules are indicated by @ and # symbols, respectively. Insets show zoomed in portions of the spectra containing the tecton signals.

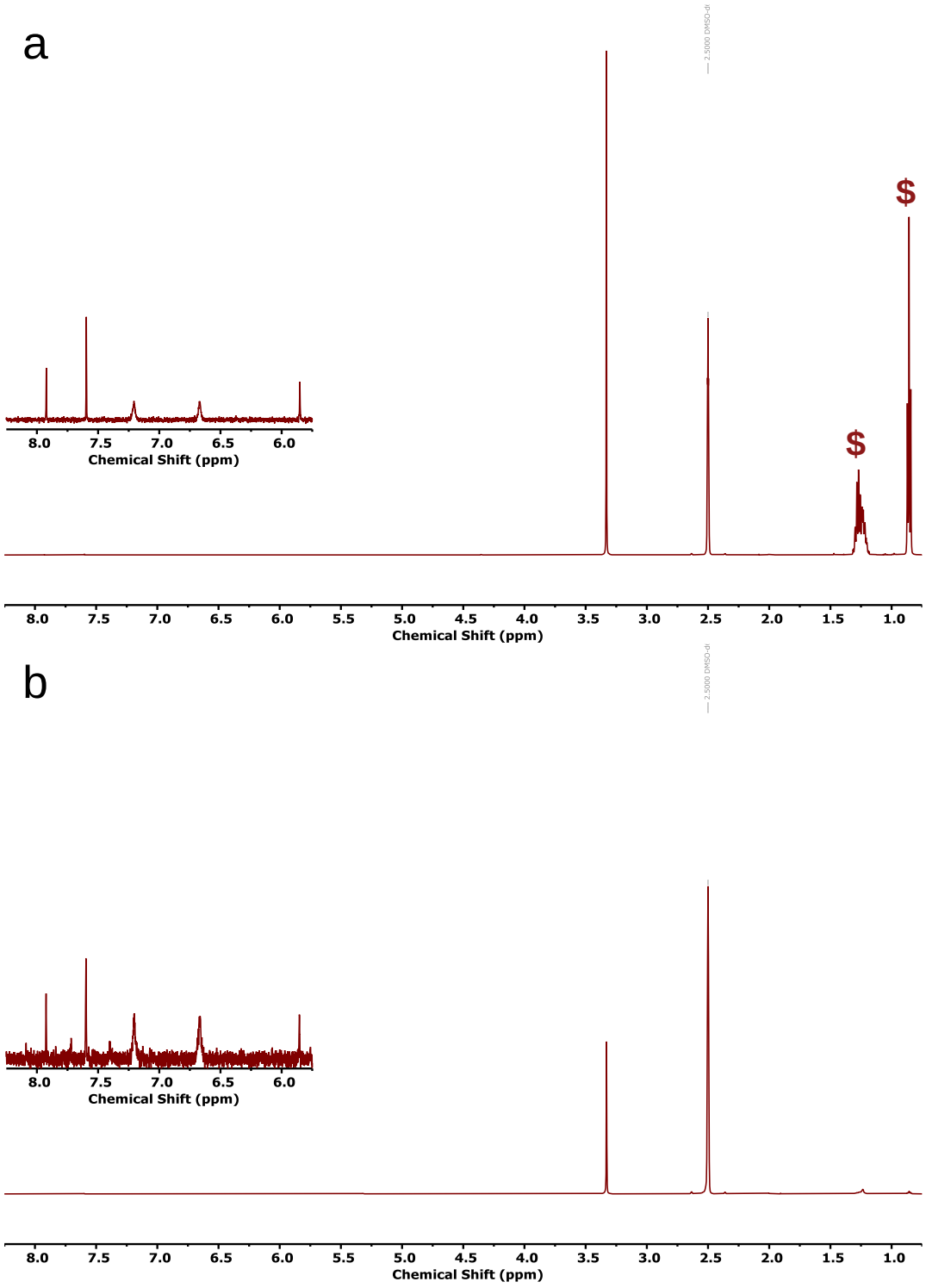

Figure S17. ^{1}H NMR spectra of **Trip1Sez2Tez**-*I* samples taken (a) after 5 exchange cycles with *n*-pentane and (b) after activation. The signals of *n*-pentane guest molecules are indicated by $ symbols. Insets show zoomed in portions of the spectra containing the tecton signals.

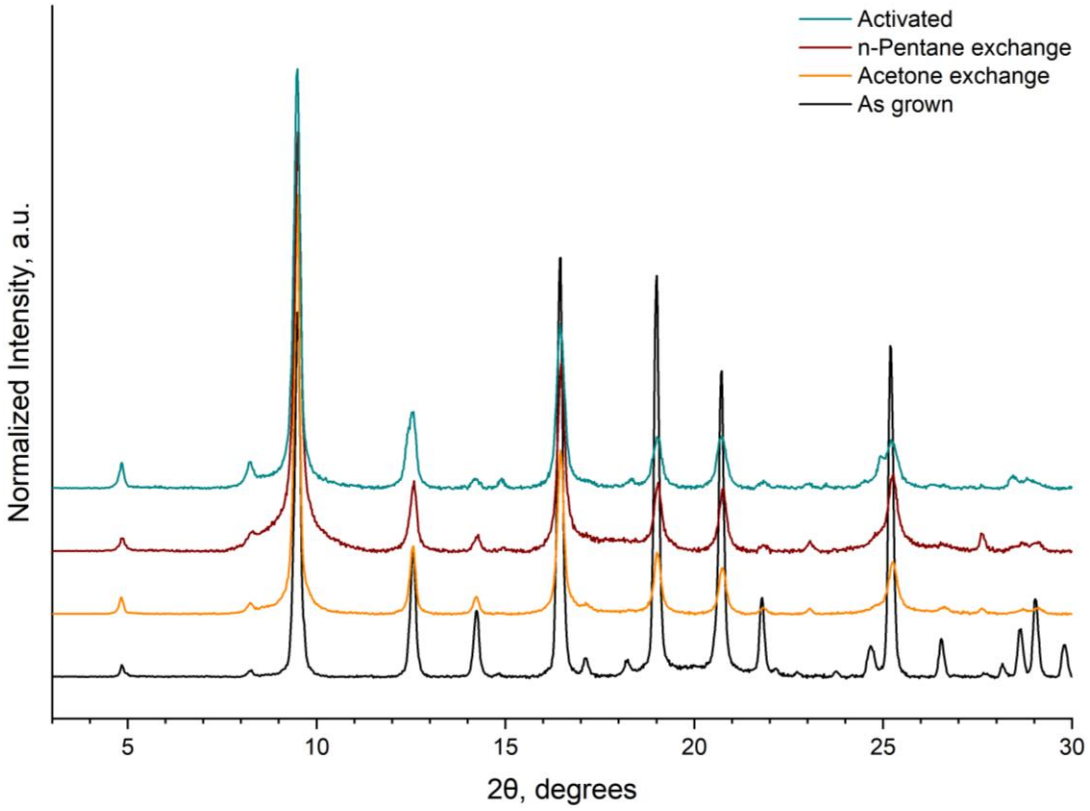

Figure S18. Stacked PXRD patterns of **Trip1Sez2Tez**-*I* samples taken as grown from DMSO, after 5 exchange cycles with acetone, after 5 exchange cycles with *n*-pentane, and after activation.

*4.2 Gas sorption measurements with **Trip2Sez1Tez**-I and **Trip1Sez2Tez**-I*

The N_2 isotherms were measured using a Micromeritics ASAP 2020 plus instrument up to a pressure of ~ 0.8 bar. Each activated sample (~ 50 mg) was placed in a pre-weighed glass measurement tube, capped with a Micromeritics TranSeal, then degassed under vacuum on the instrument overnight, reaching the detection limit (~ 4 μbar). Then the evacuated tube was removed from the instrument and weighed to determine the mass of the degassed sample. Then, the tube was transferred to the analysis port of the adsorption instrument. The isotherms were collected in a 77 K liquid N_2 bath.

Both **Trip2Sez1Tez**-*I* and **Trip1Sez2Tez**-*I* notably exhibited Type II N_2 isotherms indicating surface adsorption of non-porous or macroporous samples.[9]

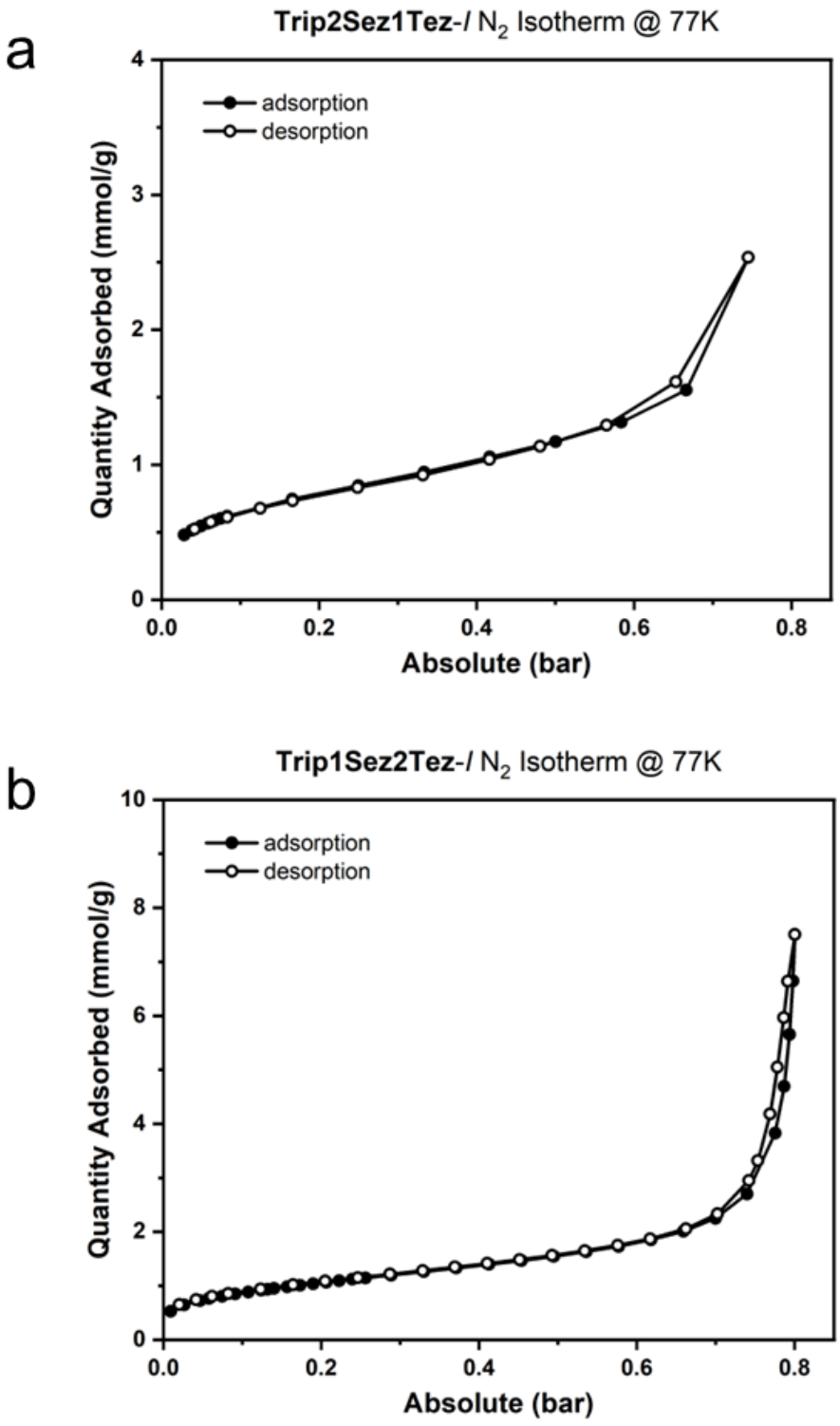

Figure S19. N_2 sorption isotherm data for (a) **Trip2Sez1Tez**-*I* and (b) **Trip1Sez2Tez**-*I*, recorded at 77 K.

S5. References

1 M. Mastalerz, S. Sieste, M. Cenić and I. M. Oppel, *The Journal of Organic Chemistry*, 2011, **76**, 6389-6393; N. G. White and M. J. MacLachlan, *The Journal of Organic Chemistry*, 2015, **80**, 8390-8397.

2 B. J. Eckstein, L. C. Brown, B. C. Noll, M. P. Moghadasnia, G. J. Balaich and C. M. McGuirk, *Journal of the American Chemical Society*, 2021, **143**, 20207-20215.

3 *Journal*, 2019.

4 G. M. Sheldrick, *Acta Crystallographica Section A Foundations and Advances*, 2015, **71**, 3-8.

5 G. M. Sheldrick, *Acta Crystallographica Section C Structural Chemistry*, 2015, **71**, 3-8.

6 O. V. Dolomanov, L. J. Bourhis, R. J. Gildea, J. A. K. Howard and H. Puschmann, *Journal of Applied Crystallography*, 2009, **42**, 339-341.

7 A. L. Spek, *Acta Crystallographica Section C Structural Chemistry*, 2015, **71**, 9-18.

8 C. F. Macrae, I. Sovago, S. J. Cottrell, P. T. A. Galek, P. McCabe, E. Pidcock, M. Platings, G. P. Shields, J. S. Stevens, M. Towler and P. A. Wood, *Journal of Applied Crystallography*, 2020, **53**, 226-235.

9 M. Thommes, K. Kaneko, A. V. Neimark, J. P. Olivier, F. Rodriguez-Reinoso, J. Rouquerol and K. S. W. Sing, *Pure and Applied Chemistry*, 2015, **87**, 1051-1069.